

# Thermal stability of $\text{Cu}_{0.3}(\text{SSe}_{20})_{0.7}$ chalcogenide glass by differential scanning calorimetry

A.A. Soliman\*

Physics Department, Faculty of Science, Ain Shams University, Abbassia-11566, Cairo, Egypt

Received 27 December 2003; received in revised form 24 April 2004; accepted 26 April 2004

Available online 9 June 2004

## Abstract

Thermal stability of  $\text{Cu}_{0.3}(\text{SSe}_{20})_{0.7}$  chalcogenide glass was investigated by differential scanning calorimetry (DSC). The level of stability for first  $\text{SSe}_{20}$  and second  $\text{Cu}_2\text{Se}$  phases of the present glass was estimated by evaluation of the glass criteria: Deitzel first glass criterion,  $\Delta T$ , Hruby criterion,  $H_r$ , and Saad and Poulain weighted thermal criteria,  $H'$  and  $S$ . The values of these criteria were obtained based on characteristic temperatures such as: the glass transition temperature,  $T_g$ , the onset temperature of crystallization,  $T_c$ , the temperature corresponding to the maximum crystallization rate,  $T_p$  and the melting temperature  $T_m$ . It was found that the values of  $\Delta T$ ,  $H_r$ ,  $H'$  and  $S$  parameters for the first  $\text{SSe}_{20}$  phase is smaller than that of the second  $\text{Cu}_2\text{Se}$  phase. That indicates a greater thermal stability of second  $\text{Cu}_2\text{Se}$  phase. The stability order at different heating rates is  $\text{Cu}_2\text{Se} > \text{SSe}_{20}$  as revealed also by thermal  $K_r(T)$  criterion.

© 2004 Elsevier B.V. All rights reserved.

**Keywords:** Thermal stability; Chalcogenide glasses; DSC

## 1. Introduction

The chalcogenide vitreous semiconductors (ChVS) have attracted much attention in the field of photo-induced effects since they exhibit photo-stimulated diffusion of metals (mainly Ag or Cu) into ChVS, which are applicable in a variety of microelectronics [1–5], optical memory [6], holography, diffractive optics [7–10] and photoresistors [11–13]. These materials must be stable in the amorphous state at low temperature and have a short crystallization time [14]. Therefore it is very important to know the glass forming ability and chemical durability of this type of materials.

In order to evaluate the level of glass stability for the investigated chalcogenide glass, different simple quantitative methods have been used. Most of these methods [15–19] are based on characteristic temperatures such as the glass transition temperature,  $T_g$ , the crystallization temperature,  $T_p$ , or the melting temperature,  $T_m$ . Some of them [20,21] are based on the reaction rate constant,  $K$ . Some of the others

[22–24] are based on crystallization activation energy. These thermal parameters [25] are easily and accurately obtained by differential scanning calorimetry (DSC) during the heating processes of glass samples. The first thorough study on the glass thermal stability of various compounds was done by Sakka and Mackenzie [26], using the ratio  $T_g/T_m$ . A parameter usually employed to estimate the glass stability is the thermal stability ( $\Delta T$ ), which is defined by  $\Delta T = T_c - T_g$  [15], where  $T_c$  is the onset temperature of crystallization. Another parameter introduced by Hruby [18] is the glass forming ability  $H_r = \Delta T / (T_m - T_p)$ , and compositional dependencies of the Hruby coefficient were survived by Sestak [27]. On the basis of the  $H_r$  parameter, Saad and Poulain obtained two other parameters, weighted thermal stability  $H' = \Delta T / T_g$  and  $S = (T_p - T_c) \Delta T / T_g$  parameter.

In the present work, the above mentioned parameters have been applied to the  $\text{Cu}_{0.3}(\text{SSe}_{20})_{0.7}$  chalcogenide glass.

## 2. Theoretical analysis

The theoretical basis for the interpretation of the DSC results is provided by the formal theory of transformation kinetics. this theory describes the evolution with time,  $t$ , of

\* Present address: Physics Department, Faculty of Science, King Khalid University, Abha-9004, Saudi Arabia. Tel.: +966 722 44935; fax: +966 722 90165.

E-mail address: [alaa.soliman2000@hotmail.com](mailto:alaa.soliman2000@hotmail.com) (A.A. Soliman).

the crystallized fraction  $\chi$  in terms of the crystalline growth rate  $u$ :

$$\chi = 1 - \exp \left[ -g \left( \int_{t'}^t u \, d\tau \right)^n \, dt' \right] = 1 - \exp(-I^n) \quad (1)$$

where  $g$  is a geometric factor which depends on the shape of the crystalline growth and  $n$  is a parameter which depends on the mechanism of transformation. It has been pointed out [28,29] that in non-isothermal measurements, generally due to a rapid temperature rise and big differences in the latent heats of nucleation and growth, the crystallization exotherm characterizes the growth of the crystalline phase from the amorphous matrix; nucleation is more or less calorimetrically unobservable at temperatures below the crystallization exotherm, or it takes place very rapidly and immediately after overheating of the material in the initial stages of the crystallization exotherm, which results in the deformed beginning of the measured exotherm. Therefore, in Eq. (1) it is assumed that the nucleation process takes place early in the transformation and nucleation rate is zero thereafter. Although, in general, the temperature dependence of the crystal growth rate is not Arrhenian when a broad range of temperature is considered [30], however, over a sufficiently limited range of temperature (such as the range of crystallization peaks in DSC experiments)  $u$  may be described in a zeroth-order approximation by

$$u = u_0 \exp \left( -\frac{E_G}{RT} \right) \quad (2)$$

where  $E_G$  is the effective activation energy for growth,  $u_0$  a pre-exponential factor and  $R$  is the ideal gas constant.

Differentiating Eq. (1) with respect to time and substituting Eq. (2) in the resulting expression, the crystallization rate is obtained as

$$\frac{d\chi}{dt} = n(1 - \chi)I^n K_0 \exp \left( -\frac{E_G}{RT} \right) = nK(1 - \chi)I^{n-1} \quad (3)$$

$K$  being the reaction rate constant.

The maximum crystallization rate in a non-isothermal process is found by making  $d^2\chi/dt^2 = 0$ , thus obtaining the relationship

$$nK_p(I^n)|_p = \alpha E_G(I)|_p/RT_p + (n - 1)K_p \quad (4)$$

where  $\alpha = dT/dt$  is the heating rate and where the quantity values which correspond to the maximum crystallization rate are denoted by subscript  $p$ . The time integral  $I$ , where

$$I = gu_0 \int_0^t e^{-(E_G/RT)} \, dt' \quad (5)$$

is transformed to a temperature integral yielding,

$$I = \left( \frac{K_0}{\alpha} \right) \int_{T_0}^{T'} e^{-(E_G/RT)} \, dT' \quad (6)$$

The integral is further transformed by substituting  $y = E_G/RT$

$$I = - \left( \frac{E_G K_0}{R\alpha} \right) \int_{y_0}^{y'} \frac{e^{-y}}{y^2} \, dy \quad (7)$$

This integral can be evaluated using the exponential integral function if it is assumed that  $T_0 \ll T'$ , so that  $y_0$  can be taken as  $\infty$ . This assumption is justifiable for any heating treatment which begins at a temperature where nucleation and crystal growth are negligible, i.e., below  $T_g$  for most glass-forming systems.

The exponential integral function,  $E(-y)$ , is represented by several approximate analytical expressions. The most convenient expression for the present problem is given by Abramovitz and Stegun [31]

$$E(-y) = \frac{-e^{-y}}{y} \left( 1 - \frac{1}{y} + \frac{2}{y^2} - \frac{6}{y^3} \dots \frac{(-1)^n n!}{y^n} \right) \quad (8)$$

when  $y_0 = \infty$ , the integral in Eq. (7) can be expressed [32] as

$$\int_{\infty}^{y'} \frac{e^{-y}}{y^2} \, dy = \frac{-e^{-y'}}{y'} - E_i(-y') \quad (9)$$

for  $y' = (E_G/RT) \gg 1$ , the integral becomes

$$\int_{\infty}^{y'} \frac{e^{-y}}{y^2} \, dy = \frac{-e^{-y'}}{y'} + \frac{e^{-y'}}{y'} \left[ 1 - \frac{1}{y'} \right] = \frac{-e^{-y'}}{y'^2} \quad (10)$$

substituting Eq. (10) in Eq. (7), one obtains

$$I = \frac{RK_0}{\alpha E_G} T^2 e^{-(E_G/RT)} = \frac{RT^2 K}{\alpha E_G} \quad (11)$$

substituting the value of  $I$  in Eq. (4), one obtains

$$(I^n)|_p = 1 \quad (12)$$

then

$$\frac{RT_p^2 K_0 e^{-(E_G/RT_p)}}{\alpha E_G} = 1 \quad (13)$$

or in logarithmic form

$$\ln \left( \frac{\alpha}{T_p^2} \right) = -\frac{E_G}{RT_p} + \ln \left( \frac{E_G}{K_0 R} \right) \quad (14)$$

This equation represents a straight line with slope,  $E_G/R$ , and intercept,  $\ln(E_G/K_0 R)$ . Then one can obtain  $E_G$ ,  $K_0$  and  $K(T)$ . It will be recalled that the method of Kissinger leads to exactly the same result. It should be noted, however, that both the method of Kissinger and that developed above are based on the inappropriate Eq. (2).

In order to evaluate the thermal stability of the investigated glass, Surinach et al. [20] introduced a  $K(T_g) = K_0 \exp(-E_G/RT_g)$  parameter, and Hu et al. [21] developed the  $K(T_p) = K_0 \exp(-E_G/RT_p)$  parameters. Thus the values of these two parameters indicate the tendency of glass to devitrify on heating. The larger their values, the greater are the tendency to devitrify. The formation of a glass is a kinetic process. It is reasonable to assess the glass stability by a kinetic parameter,  $K(T)$ . The  $H_r$  parameter itself is a

stability factor based on characteristic temperatures. Here a stability parameter is defined as  $K_r(T)$ :

$$K_r(T) = K_o \exp\left(-\frac{H_r E_G}{RT}\right) \quad (15)$$

where  $T$  is any temperature between  $T_g$  and  $T_p$ . The smaller the values of  $K_r(T)$ , the greater are the thermal stability of the glass. The obvious advantage of this method is that it can evaluate the glass stability over a broad temperature range other than at only one temperature such as  $T_g$  or  $T_p$ .

### 3. Experimental procedure

The  $\text{Cu}_{0.3}(\text{SSe}_{20})_{0.7}$  chalcogenide glass was prepared by the quenching technique. Materials (99.999% pure) were weighted according to their atomic percentage and were sealed in a silica ampoule (length 15 cm, internal diameter 8 mm) with a vacuum  $\sim 10^{-3}$  Pa. The ampoule was kept in a furnace and heated up to  $950^\circ\text{C}$  at a rate of  $4\text{--}5^\circ\text{C}/\text{min}$ . After that, ampoule was rocked frequently for 4 h at the maximum temperature to make the melt homogeneous. Quenching was done in ice–water. The amorphous nature and purity of prepared material was checked by X-ray diffraction (XRD) using X-ray diffractometer (Philips X'pert) in the range  $18\text{--}90^\circ$  in  $0.03^\circ$   $2\theta$  steps with a counting time of 15 per step with Cu  $K\alpha$  radiation with graphite monochromator in the diffracted beam.

Differential scanning calorimetry (DSC) experiments presented in this paper were performed using a Shimadzu DSC-50 instrument on samples of  $\approx 15$  mg encapsulated in conventional platinum sample pans in an atmosphere of dry nitrogen at a flow of 30 ml/min. The instrument was calibrated with In, Pb, and Zn standards. The calorimetric sensitivity was  $10 \mu\text{W cm}^{-1}$  and the temperature precision was  $\pm 0.01$  K. Non-isothermal DSC curves were obtained with selected heating rates  $2\text{--}30$  K/min in the range  $300\text{--}873$  K. The values of the glass transition temperature ( $T_g$ ), the onset temperature of crystallization ( $T_c$ ), the peak temperature of crystallization ( $T_p$ ) and the melting temperature ( $T_m$ ) were determined by using the microprocessor of the apparatus.

### 4. Results and discussion

Fig. 1 shows X-ray diffraction patterns for the as-prepared  $\text{Cu}_{0.3}(\text{SSe}_{20})_{0.7}$  chalcogenide glass and fully crystallized glass after annealing for 24 h at 773 K. Fig. 1a confirming the glassy (amorphous) nature of the prepared glass. By analyzing the precipitated crystalline phases after crystallization (see Fig. 1b) it is confirmed that the  $\text{Cu}_{0.3}(\text{SSe}_{20})_{0.7}$  glass is crystallized in  $\text{SSe}_{20}$  and  $\text{Cu}_2\text{Se}$  phases.

Fig. 2 shows a typical differential scanning calorimetry (DSC) thermogram for the as-prepared  $\text{Cu}_{0.3}(\text{SSe}_{20})_{0.7}$  glass at a heating rate of 10 K/min. The characteristic phenomena (endothermic and exothermic peaks) are evident in

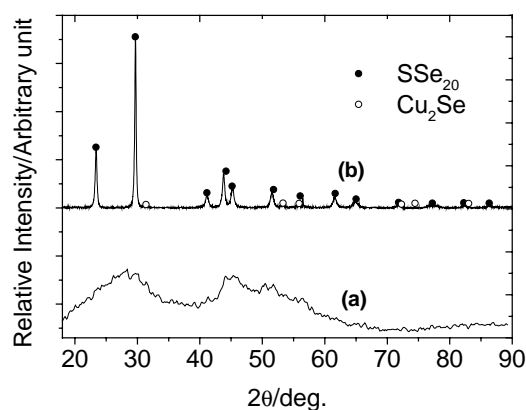


Fig. 1. X-ray diffraction patterns of  $\text{Cu}_{0.3}(\text{SSe}_{20})_{0.7}$  chalcogenide glass: (a) as-prepared glass and (b) after crystallization.

the DSC curves in the temperature range of investigation. From the analysis point of view, The DSC curve of the investigated  $\text{Cu}_{0.3}(\text{SSe}_{20})_{0.7}$  glass is divided into three parts, the first one corresponds to the glass transition region which appears as one endothermic reaction at temperature  $T_g$ , the second part is related to the crystallization process of the considered glass indicated by two exothermic crystallization peaks ( $T_{p1}$  and  $T_{p2}$ ) and the last corresponds to the melting region which appears as an endothermic reaction at temperature  $T_m$ . The glass transition temperature,  $T_g$ , the onset temperatures of crystallization ( $T_{c1}$  and  $T_{c2}$ ) and the melting temperature  $T_m$  have been defined as temperatures corresponding to the intersection of two linear portions adjoining the transition elbow of the DSC trace in the endothermic and exothermic directions (see Fig. 2). The peak temperature of crystallization ( $T_{p1}$  and  $T_{p2}$ ) is the temperature at which the crystallization attains its maximum value and considered to be the peak temperature of the exothermic reaction in DSC curve. Values of the characteristic temperatures,  $T_g$ ,  $T_c$ ,  $T_p$  and  $T_m$  for the investigated  $\text{Cu}_{0.3}(\text{SSe}_{20})_{0.7}$  glass are given in Table 1 as a function of heating rates ( $\alpha$ ). The table reveals that these values are shifted to higher values by increasing the heating rate. The glass forming ability of the

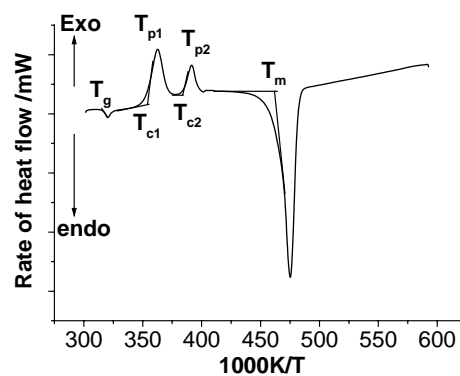


Fig. 2. Typical DSC trace of  $\text{Cu}_{0.3}(\text{SSe}_{20})_{0.7}$  chalcogenide glass at a heating rate of 10 K/min.

Table 1  
Characteristic parameters for the crystallization of the  $\text{Cu}_{0.3}(\text{SSe}_{20})_{0.7}$  chalcogenide glass

	Heating rate $\alpha$ (K/min)						
	2	5	10	15	20	25	30
Glass transition $T_g$ (K)	309.4	313.4	316.5	318.6	319.7	320.8	321.6
Melting temperature $T_m$ (K)	464.7	465.2	465.6	467.4	467.7	468.3	469.4
First peak							
$T_c$ (K)	342.0	348.1	352.9	356.6	359.1	360.3	361.9
$T_p$ (K)	349.8	356.7	362.5	357.7	370.9	371.7	374.3
$\Delta T$ (K)	32.60	34.70	36.40	38.00	39.40	39.50	40.30
$H_r$	0.284	0.320	0.353	0.381	0.407	0.409	0.424
$H'$	0.105	0.111	0.115	0.119	0.123	0.123	0.125
$S$ (K)	0.819	0.955	1.104	1.321	1.451	1.402	1.550
Second peak							
$T_c$ (K)	375.3	380.5	385.6	388.8	390.9	392.3	393.8
$T_p$ (K)	381.9	386.8	391.9	395.4	397.2	398.6	399.7
$\Delta T$ (K)	65.90	67.10	69.10	70.20	71.20	71.50	72.20
$H_r$	0.796	0.856	0.938	0.989	1.010	1.026	1.036
$H'$	0.202	0.214	0.218	0.220	0.223	0.223	0.225
$S$ (K)	1.327	1.348	1.373	1.452	1.405	1.411	1.421

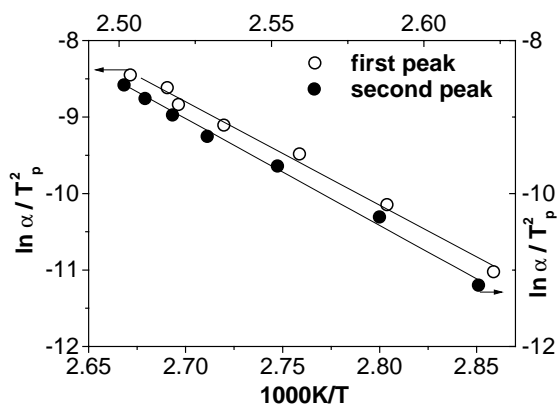


Fig. 3. Plots of  $\ln(\alpha/T_p^2)$  vs.  $1000/T_p$  and straight regression lines for the two peaks of  $\text{Cu}_{0.3}(\text{SSe}_{20})_{0.7}$  chalcogenide glass.

studied glass can be estimated by using these characteristic temperatures. The existing stability parameters are also listed in Table 1.

To obtain the kinetic parameters of the crystallization, Eq. (14) is applied. Fig. 3 shows the plot of  $\ln(\alpha/T_p^2)$  versus  $1/T_p$  for the two peaks of the  $\text{Cu}_{0.3}(\text{SSe}_{20})_{0.7}$  glass. The activation energy for growth,  $E_G$ , and frequency factor,  $K_0$ , are then evaluated by least-square fitting method. Table 2 summarizes the values determined by these calculations for the two peaks. After knowing the values of  $E_G$  and  $K_0$ , the

Table 2  
Kinetic parameters of the analyzed glass obtained from Kissinger plots

$E_G$ (kJ/mol)		$\ln K_0$ ( $\text{s}^{-1}$ )	
First peak	Second peak	First peak	Second peak
$112.34 \pm 4.32$	$182.56 \pm 3.24$	37.19	56.35

kinetic parameters  $K(T)$  and  $K_r(T)$  for the two peaks of the studied chalcogenide glass were calculated by using the relationship  $K(T) = K_0 \exp(-E_G/RT)$  and Eq. (15), respectively. The values of  $K(T)$  and  $K_r(T)$  for the temperatures  $T_g$  and  $T_p$  are listed in Table 3. Fig. 4 represents the plots of  $K_r(T)$  versus  $T$  at three different heating rates 2, 15 and 30 K/min for the two phases of the  $\text{Cu}_{0.3}(\text{SSe}_{20})_{0.7}$  glass.

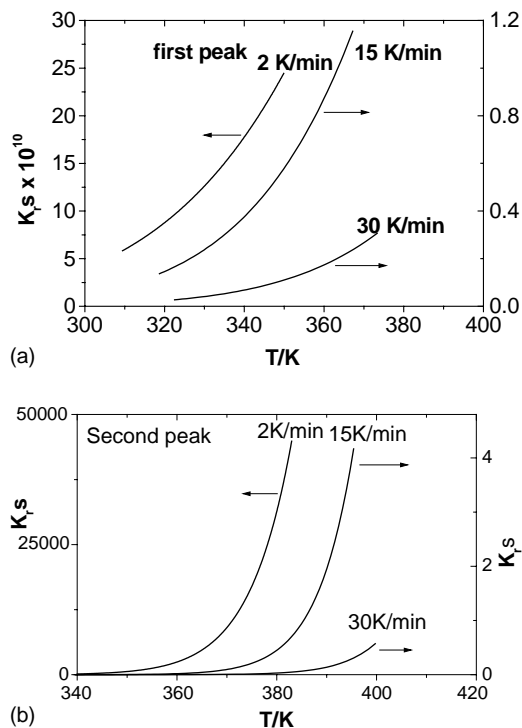


Fig. 4. Plots of  $K_r(T)$  vs.  $T$  for  $\text{Cu}_{0.3}(\text{SSe}_{20})_{0.7}$  chalcogenide glass at three different heating rates to verify the stable order: (a) first peak and (b) second peak.

Table 3  
Kinetic parameters  $K(T)$  and  $K_r(T)$  for the  $\text{Cu}_{0.3}(\text{SSe}_{20})_{0.7}$  chalcogenide glass

	Heating rate $\alpha$ (K/min)						
	2	5	10	15	20	25	30
First peak							
$K(T_g)$ ( $10^{-3} \text{ s}^{-1}$ )	1.534	2.678	4.085	5.413	6.263	7.240	8.040
$K(T_p)$ ( $\text{s}^{-1}$ )	0.238	0.502	0.924	1.559	2.141	2.316	2.981
$K_r(T_g)$ ( $10^{10} \text{ s}^{-1}$ )	5.809	1.447	4.048	1.364	4.804	4.684	2.603
$K_r(T_g)$ ( $10^{10} \text{ s}^{-1}$ )	24.43	7.723	2.740	1.180	0.516	0.496	0.320
Second peak							
$K(T_g)$ ( $10^{-6} \text{ s}^{-1}$ )	0.447	1.106	2.198	3.472	4.401	5.569	6.604
$K(T_p)$ ( $\text{s}^{-1}$ )	0.318	0.658	1.377	2.261	2.908	3.532	4.109
$K_r(T_g)$ ( $\text{s}^{-1}$ )	0.867	0.027	$1.622 \times 10^{-4}$	$7.41 \times 10^{-6}$	$2.21 \times 10^{-7}$	$9.39 \times 10^{-7}$	$5.65 \times 10^{-7}$
$K_r(T_g)$ ( $10^3 \text{ s}^{-1}$ )	3.943	2.335	44.43	4.170	1.673	0.843	0.568

It found that  $K_r(T)$  of the first  $\text{SSe}_{20}$  phase at heating rates 15 and 30 K/min varies slowly with increasing temperature  $T$  and the values are not on the  $T$  axis, indicating a relatively high stability while  $K_r(T)$  at the heating rate 2 K/min varies more rapidly with increasing  $T$ , which signifies a minor stability. The same trend of  $K_r(T)$  versus  $T$  is observed for the second  $\text{Cu}_2\text{Se}$  phase except the values of  $K_r(T)$  are on the  $T$  axis and of smaller order. Therefore, one can conclude that the second  $\text{Cu}_2\text{Se}$  phase is more thermally stable than the first  $\text{SSe}_{20}$  phase.

It is known that these existing parameters of glass stability allow to predict the glass forming ability of a material [14]. It is possible to suggest that the larger their values, the greater should be the glass thermal stability. According to these suggestions, the parameters,  $\Delta T$ ,  $H_r$ ,  $H'$  and  $S$ , in Table 1 show that the second  $\text{Cu}_2\text{Se}$  phase is more stable than the first  $\text{SSe}_{20}$  phase. Also, it is possible to obtain a consistent stable order for these two glass phases by the reaction rate constant. According to the literature [20,21], the smaller the values of  $K(T_g)$  and  $K(T_p)$  parameters, the better should be the glass forming ability of the material. In spite of  $K(T_g)$  and  $K(T_p)$  values in Table 3 indicate that the second  $\text{Cu}_2\text{Se}$  phase is more stable than the first  $\text{SSe}_{20}$  phase, and the stability order at the three different heating rates is  $\text{Cu}_2\text{Se}$  phase >  $\text{SSe}_{20}$  phase. In addition, by using Eq. (15), the data of  $K_r(T_g)$  and  $K_r(T_p)$  were calculated and listed in Table 3, showing that the second  $\text{Cu}_2\text{Se}$  phase is also the more stable, and the order of stability is also  $\text{Cu}_2\text{Se}$  phase >  $\text{SSe}_{20}$  phase at the three heating rates. This stability result agrees with that of the  $K(T_g)$  and  $K(T_p)$  parameters.

## 5. Conclusion

The characteristic temperatures of  $\text{Cu}_{0.3}(\text{SSe}_{20})_{0.7}$  chalcogenide glass has been performed to evaluate the glass forming ability of its two phases by using various thermal stability parameters. The  $K_r(T)$  parameter allowed to evaluate the glass stability over a broad temperature range from

$T_g$  to  $T_p$  and at different heating rates. It is found that, all the thermal stability parameters are affected both by the heating rate and by temperature. The second  $\text{Cu}_2\text{Se}$  phase is more stable than the first  $\text{SSe}_{20}$  phase. Finally the stability order of these two phases is  $\text{Cu}_2\text{Se}$  phase >  $\text{SSe}_{20}$  phase.

## References

- [1] Z.K. Heiba, M.B. El-Der, K. El-Sayed, Powder Diffr. 17 (2002) 191.
- [2] Y. Mizushima, A. Yoshikawa, in: Y. Hamakawa (Ed.), Amorphous Semiconductors Technology and Devices, OHM, Tokyo, North-Holland, Amsterdam, 1982, p. 277.
- [3] E. Shepeljavi, A.V. Stronski, I.Z. Indutnyi, in: Proceedings of Ukrainian Vacuum Society, vol. 1, IMF NASU, Kiev, 1995, p. 324.
- [4] I.Z. Indutnyi, S.A. Kostioukevitch, A.V. Stronski, P.E. Shepeljavi, Optics as a key to High technology, in: T. Lippeny, G. Lupkovits, A. Podmaniczky (Eds.), Gy. Akos. Proc. SPIE, vol. 1983, part 1, 1993, p. 464.
- [5] A.V. Stronski, in: G. Harman, P. Mach (Eds.), Microelectronic Interconnections and Assembly, NATO ASI Series 3: High Technology, vol. 54, 1998, p. 263.
- [6] I.Z. Indutnyi, P.E. Shepeljavi, P.F. Romanenko, I.I. Robur, A.V. Stronski, in: V.V. Petrov, S.V. Svechnikov (Eds.), Proceeding of SPIE, Optical Storage, Imaging and Transmission of Information, vol. 3055, 1996, p. 50.
- [7] A.V. Stronski, M. Vlcek, J. Prokop, T. Wagner, S.A. Kostioukevitch, P.E. Shepeljavi, Proc. Ukrainian Vac. Soc. 3 (1997) 235.
- [8] I.Z. Indutnyi, M.T. Kostishin, P.F. Romanenko, A.V. Stronski, J. Inf. Rec. Mats. 19 (1991) 251.
- [9] P.E. Shepeljavi, S.A. Kostioukevitch, I.Z. Indutnyi, A.V. Stronski, in: M. Tabib-Azar, D.L. Polla, K. Wong (Eds.), Proceeding of SPIE, Integrated Optics and Microstructures II, vol. 2291, 1994, p. 188.
- [10] I.Z. Indutnyi, A.V. Stronski, S.A. Kostioukevitch, P.F. Romanenko, P.E. Shepeljavi, I.I. Robur, Opt. Eng. 34 (1995) 1030.
- [11] J.A. Savage, Infrared Optical Materials and Their Antireflection Coatings, Adam Hiliger, Bristol, 1985.
- [12] Z. Cimpl, F. Kosek, J. Non-Cryst. Solids 90 (1987) 577.
- [13] A.B. Seddon, M.J. Laine, J. Non-Cryst. Solids 213 (1997) 168.
- [14] J. Vázquez, P.L. López-Alemay, P. Villares, R. Jiménez-Garay, J. Alloys Compd. 354 (2003) 153.
- [15] A. Dietzel, Glasstech. Ber. 22 (1968) 1187.
- [16] D.R. Uhlmann, J. Non-Cryst. Solids 7 (1972) 337.
- [17] D.R. Uhlmann, J. Non-Cryst. Solids 25 (1977) 43.
- [18] A. Hruby, Czech. J. Phys. B 22 (1972) 187.

- [19] M. Saad, M. Poulain, *Mater. Sci. Forum* 19–20 (1987) 11.
- [20] S. Surinach, M.D. Baro, M.T. Clavaguera-Mora, N. Clavaguera, *J. Mater. Sci.* 19 (1984) 3005.
- [21] L. Hu, Z. Jiang, *J. Chin. Ceram. Soc.* 18 (1990) 315.
- [22] A. Marotta, A. Buri, F. Branda, *J. Non-Cryst. Solids* 95–96 (1987) 593.
- [23] X. Zhao, S. Sakka, *J. Non-Cryst. Solids* 95–96 (1987) 487.
- [24] F. Branda, A. Marotta, A. Buri, *J. Non-Cryst. Solids* 134 (1991) 123.
- [25] J. Málek, *J. Non-Cryst. Solids* 107 (1988) 323.
- [26] S. Sakka, J.D. Mackenzie, *J. Non-Cryst. Solids* 6 (1971) 145.
- [27] J. Sestak, *J. Therm. Anal.* 33 (1988) 75.
- [28] E. Illekova, *J. Non-Cryst. Solids* 68 (1984) 153.
- [29] A.A. Soliman, S. Al-Heniti, A. Al-Hajry, M. Al-Assiri, G. Al-Barakati, *Thermochim. Acta* 413 (2004) 57–62.
- [30] J. Vázquez, P.L. López-Alemay, P. Villares, R. Jiménez-Garay, *Acta Mater.* 44 (1996) 4807.
- [31] M. Abramowitz, I.E. Stegun, *Handbook of Mathematical Functions*, Dover, New York, 1972.
- [32] I.S. Gradshteyn, I.M. Ryzhik, *Tables of Integrals, Series and Products*, Academic Press, New York, 1972.